Phosphorylation Status of Peptide Monolayers Modulates Hydrogen Bonding and Orientations of Nematic Liquid Crystals

Reza Abbasi [a], Chenxuan Wang [a], Yiqun Bai [a], and Nicholas L. Abbott [a]*

[a] *Department of Chemical and Biological Engineering, University of Wisconsin–Madison, Madison, USA*

*corresponding author: abbott@engr.wisc.edu

This supporting information contains details of materials and experimental methods used in this study and figures and tables which demonstrate the results of characterization of dipeptide and tripeptide decorated surfaces using X-ray photoelectron spectroscopy (XPS), chemical force microscopy (CFM) and cyclic voltammetry. One section is dedicated to Johnson-Kendall-Roberts (JKR) theory of adhesion mechanics and its application to calculate the mean adhesion force per EG4 molecule for hydrogen bonding surfaces.

Materials and Experimental Methods

Materials

Unless noted otherwise, all materials were used as received. Silicon wafers were purchased from Silicon Sense (Nashua, NH). Glass slides (1'' x 3'') were cut from sheets of Corning Eagle 2000 glass from Delta Technologies (Stillwater, MN). Gold (99.999% purity) was obtained from International Advanced Materials (Spring Valley, NY). Titanium (99.99% purity) was obtained from PureTech (Brewster, NY). 1-decanethiol ($C_{10}SH$), 1-dodecanethiol ($C_{12}SH$), 1-pentadecanethiol ($C_{15}SH$), 1-hexadecanethiol ($C_{16}SH$), tetra-ethylene glycol thiol terminated in

hydroxyl group (EG4) (HS-$(CH_2)_{11}$-EG_4-OH), triethylamine, triethanolamine and tetradecane ($C_{14}H_{30}$) (purity>=99%) were purchased from Sigma-Aldrich (Milwaukee, WI). Liquid crystals 4-cyano-4'-pentylbiphenyl (5CB) and TL205 were obtained from EMD (Hawthorne, NY). TL205 is a mixture of mesogens containing cyclohexane-fluorinated biphenyls and fluorinated terphenyls with aliphatic chains containing 2-5 carbons.[1, 2] Anhydrous ethanol containing 5% isopropyl alcohol and 5% methanol as denaturants was obtained from Sigma-Aldrich (Milwaukee, WI) and purged with argon gas for at least 1 hour prior to use. Poly (dimethylsiloxane) (PDMS) stamps were prepared using a Sylgard 184 silicone elastomer kit obtained from Dow Corning (Midland, MI). Peptides were purchased from New England Peptide (Gardner, MA) with end group protection acetylated N-termini and amidated C-termini (all of the peptides used in this study consist of L-amino acids). We used end group protection to eliminate potential changes in the extent of ionization of the terminal amine and carboxylic acid groups of unprotected peptides.[1, 3] Matrix-assisted laser desorption ionization time-of-flight (MALDI-TOF) analysis was reported by New England Peptide to be within 0.1% of the calculated molecular weight. The purity of the peptides was found to be > 95%, as determined by analytical high-performance liquid chromatography (HPLC).

Preparation of Gold Coated Glass Substrates

Briefly, piranha-cleaned glass slides were positioned within the chamber of an electron-beam evaporator (VES-3000-C manufactured by Tek-Vac Industries, Brentwood, NY) such that the angle (θ_i, with respect to the surface normal) at which both titanium (Ti) and gold (Au) were deposited onto the glass slides was specified with an accuracy of ±1°. Semitransparent gold films (used for optical measurements of LC orientations) were prepared by sequentially depositing 8

nm of Ti and 20 nm of Au. The films were deposited at an angle of incidence of 35° ± 1°. Reflective gold films that were prepared by depositing 100 nm of Au on silicon wafers were used for ellipsometry, X-ray photoelectron spectroscopy (XPS), polarization modulation-infrared reflection absorption spectroscopy (PM-IRRAS) and cyclic voltammetry measurements. The latter films were deposited at normal incidence. All gold films were used within 1 hour of removal from the evaporator chamber.[1]

Preparation of Peptide-Modified Gold Coated Glass Surfaces

Prior to formation of monolayer of peptides on the gold films, monolayers formed from hexadecanethiol ($C_{16}SH$) were patterned onto the edge regions of the gold films by using microcontact printing. The monolayers formed from $C_{16}SH$ (i) served to confine droplets of the peptides placed onto the gold films, and (ii) served as reference regions on the surfaces for quantifying the orientations of the LCs. The peptides were generally prepared in aqueous 100 mM triethanolamine buffer (pH 7.2, 500 μM peptide) and droplets of the peptide solution were placed by hand pipetting on the gold film and incubated on the gold films for 23 hours. After incubation, the surfaces were rinsed sequentially in deionized water, aqueous HCl (pH 4.2) and then deionized water (pH 5-6). We used the aqueous HCl solution to rinse the gold films because we have observed that acidic solutions aid in the removal of peptides bound to surfaces through physical interactions.[1]

Fabrication of Optical Cells

Optical cells used for quantification of the orientation of the LCs on peptide-modified gold films were fabricated by pairing each peptide-modified surface with a reference surface. The reference surface was a gold film (deposited at an angle of 64° relative to the surface normal) that

was functionalized with a 1 mM ethanolic solution of pentadecanethiol ($C_{15}SH$) for 23 hours. The reference surface was selected to strongly anchor nematic 5CB in an azimuthal direction that was perpendicular to the direction of incidence of the gold during deposition of the gold films. The peptide-decorated surfaces and reference surfaces were spaced apart using polyethylene terephthalate (PET) spacers with a thickness of 50 μm. Both 5CB and TL205 were gradually heated to (36°C) (the clearing temperature of 5CB) and then drawn into the cavity between the two surfaces via capillary action. The samples were then gradually cooled to room temperature (25°C) prior to imaging.[1]

Measurement of the Orientations of LCs

In the measurements reported in this paper, the azimuthal orientation of the LCs at the peptide decorated surface of the optical cell differed from that at the reference surface (both surfaces caused planar anchoring of the LCs). These boundary conditions induced a twist distortion in the LC and we define the twist angle of the LC as the change in the azimuthal orientation of the director of the LC upon moving from the reference surface to the peptide- decorated surface. As detailed previously,[1] we measured the twist angle (ψ) at each pixel of a polarized light micrograph (transmission mode) of the film of LC by rotating the analyzer and polarizer so as to minimize the transmission of light through each pixel. A color map of the twist angles of the LC measured across each sample was constructed by assigning a specific color to each value of the twist angle [1]. In this paper, we report the azimuthal orientation of the LCs on the peptide-decorated regions of the surface as the difference between the twist angles of the LCs on the peptide- and $C_{16}SH$-decorated regions of the top surface of the optical cell (the orientation of LCs on gold films with a monolayer of $C_{16}SH$ corresponds to the direction of gold deposition on the top surface of the optical cell).

We note that the small difference in the exact angles measured between this study and our previous study [1] results from the use of two separate batches of 5CB. We have noticed small batch-to-batch variations (~2°) in the quantitative angles measured by using different batches of 5CB. Therefore, the results reported in this paper were all obtained from the same batch of 5CB. Here, we emphasize that the orientations of the LCs on the peptide-decorated surfaces investigated in this paper were highly reproducible. Error bars reported for twist angle values represent the standard error of the mean for at least thirty measurements (i.e. thirty different spots that were functionalized with a monolayer of each specific peptide being investigated) done on two separate batches of gold films.

Ellipsometry Measurements

The optical thicknesses of the monolayers formed by peptides on 100 nm-thick films of gold were determined using a Rudolph AutoEL II ellipsometer (wavelength 632 nm, angle of incidence 70^{o}, Rudolph Tech., Flanders, NJ). The average thickness was determined by measuring three locations on three samples. Error bars represent the standard error of the mean over the nine measurements. The ellipsometric constants of each batch of gold films were determined by performing ellipsometric measurements on a piece of a gold film on which a monolayer of $C_{16}SH$ was formed. By using the optical thickness of $C_{16}SH$ monolayer reported in the literature (2.3nm) [4], the ellipsometric constants of the gold films were calculated. For the calculation of the optical thickness of a peptide monolayers, the refractive index was assumed to be $n = 1.46$.[1]

X-ray Photoelectron Spectroscopy (XPS) Measurements

XPS was used to determine the atomic composition and to compare the surface coverages of the dipeptide and tripeptide decorated surfaces. The instrument that was used for our

measurements was a Thermo Fisher Scientific (Waltham, Massachusetts) K-Alpha™ (XPS) system that was equipped with monochromatic and micro-focused Al K-Alpha X-ray source. The XPS spectra were collected over a surface area of approximately (400 μm× 600 μm). Survey scans with a pass energy of 200 eV were first performed to identify the elements that were present on the surface, followed by acquisition of element-specific spectra with a pass energy of 50 eV. The major peaks of interest were Au (4f), O (1s), C (1s), N (1s), and S (2p).The percentage composition of each element that was present on the surface was determined, after establishment of baselines, by integrating the area under the corresponding peaks of that element and correcting for the element specific sensitivity factors.[1, 5]

Polarization Modulation-Infrared Reflection Absorption Spectroscopy Measurements

Infrared spectra of the dipeptide and tripeptide monolayers formed on gold films (thickness of 100 nm) were obtained using a NicoletMagna-IR 860 FT-IR spectrometer with a photoelastic modulator (PEM-90, Hinds Instruments, Hillsboro, OR), a synchronous sampling demodulator (SSD-100, GWC Technologies, Madison, WI) and a liquid N_2-cooled mercury cadmium telluride (MCT) detector. All spectra were taken at an incident angle of 83° with the modulator centered at 1600 cm^{-1}. Three independent samples were analyzed (for each sample, 1000 scans were taken at a resolution of 2 cm^{-1}). The spectrum presented in this manuscript for each peptide-decorated surface is the average of the three spectra collected this way. OMNIC software (Thermo Fisher Scientific; Waltham, MA) was used to normalize the baselines.

Preparation of Gold Coated Silicon Substrates and AFM Tips

Silicon wafers and AFM tips were coated with a 2 nm layer of titanium (Ti) and a 20 nm layer of gold (Au) at normal incidence using an electron beam evaporator (VES-3000-C manufactured by Tek-Vac Industries, Brentwood, NY). All gold coated silicon substrates and AFM tips were used within 1 hour of removal from the evaporator chamber.[1, 5]

Preparation of Chemically Modified AFM Tips

Following gold deposition, the gold coated AFM tips were immersed in a 1 mM ethanolic solution of either 1-dodecanethiol or EG4 and incubated for at least 23 hours. Upon removal of AFM tips from the solution and before use, the tips were rinsed carefully by ethanol and then dried in a gentle stream of nitrogen.[5]

Preparation of Peptide-Decorated Surfaces for Adhesion Force Measurements

Following gold deposition, the gold coated silicon substrates were cut in to small pieces and then immersed in peptide solutions (100 mM triethanolamine buffer, pH 7.2, 500 μM peptide) and incubated for at least 23 hours. After incubation, the substrates were rinsed sequentially in deionized water, aqueous HCl (pH 4.2), deionized water (pH 5-6) and then dried gently in a stream of N_2.[1, 5]

Adhesion Force Measurements

Adhesion force measurements were conducted using a Multimode IIIa SPM system (Bruker, (Elk Grove Village, Illinois)) under tetradecane or methanol solution using chemically modified AFM tips (tips were purchased from Bruker, (Elk Grove Village, Illinois))). The spring constants of the cantilevers were measured using the thermal tuning method on a Nanoscope V

Multimode AFM and determined to be 0.088±0.014 N/m (nominally 0.03 N/m). Contact time was kept constant at 500 ms, and the approaching rate was kept constant at 1000 nm/s. In order to get accurate and reliable adhesion force data, at least three independent tip-sample combinations were used [6]. In addition, force curves were recorded by moving the functionalized AFM tip over at least three different spots on each sample and at least 330 force curves were recorded at each spot. Therefore, at least 3000 force curves were used to plot the adhesion force histograms presented in this paper [5]. The values reported for the error bars of the mean adhesion force represent the standard error of the mean over at least 3000 adhesion force measurements.

Cyclic Voltammetry Measurements

Cyclic voltammetry was performed using a Pine Instruments AFCBP1 bipotentiostat (Grove City, PA). The electrochemical cell was arranged in a standard three-electrode configuration using a peptide monolayer formed on gold film (thickness of 100 nm) as working electrode, a platinum wire mesh as counter electrode and a Ag/AgCl reference electrode (BASi, West Lafayette, IN). Cyclic voltammograms were acquired in 0.5 M KCl (the solution pH was adjusted to be 8.5 using KOH) by scanning between -1.4 V and -0.5 V with respect to the standard Ag/AgCl reference electrode at 100 mV/s. All experiments were performed at room temperature (approximately 25 °C) after deaerating the electrolyte solution with ultrapure N_2 gas for at least 30 min. The desorption peak potentials and desorption peak areas were calculated after baseline subtraction. The surface coverage was estimated by converting the entire area under the desorption curve into charge. The baseline corrected voltammogram presented in the manuscript for each peptide monolayer is the average from at least three independent samples.

Characterization of Peptide-Decorated Surfaces using XPS

Figure S1 and S2 show XPS spectra and detailed atomic composition information for the non-phosphorylated peptides. **Figure S3** shows Au (4f) and S (2p) spectra and calculated peak areas corresponding to Au (4f) and S (2p) peaks.

Characterization of Peptide-Decorated Surfaces using PM-IRRAS

Figure S4, S5, S6, and S7 show PM-IRRAS spectra for all non-phosphorylated and phosphorylated peptide monolayers (see **Table S1** for peak assignments). Close inspection of the **Figure S4, S5, S6, S7** and **Table S1** reveals two key observations. Firstly, the presence of vibrational modes in the absorption spectra corresponding to the amide I, amide II, methyl rocking and C-C stretching and aromatic ring of tyrosine absorption energies confirms the formation of monolayers of peptides on gold films. Secondly, we cannot detect any spectroscopic signature of free (i.e. non-hydrogen bonded) or hydrogen bonded hydroxyl (-OH) groups in the PM-IRRAS spectra of peptide monolayers, which we believe is a result of limits in instrument sensitivity (free (-OH) group shows a relatively sharp but weak stretching peak around 3350 cm^{-1} [7, 8] and hydrogen bonded (-OH) group shows a very wide and weak stretching peak around 3250 cm^{-1} [7, 8]; none of these peaks are observable in the PM-IRRAS spectra of peptide monolayers).

Calculating the Mean Adhesion Force per EG4 Molecule using Johnson-Kendall-Roberts (JKR) Theory of Adhesion Mechanics

The (JKR) [9] theory describes the adhesion between a spherical tip and a flat substrate in a surrounding medium. The magnitude of mean adhesion force ($F_{Adhesion}$) is given by the following formula:

$$F_{Adhesion} = \left(\frac{3}{2}\right)\pi R W_{Adhesion} \quad (1)$$

Where R is radius of curvature of the AFM tip (in our case we have estimated R as 53 ± 5 nm from scanning electron microscopy (SEM) image (data not shown)) and $W_{Adhesion}$ is the work of adhesion (i.e. the work required to pull the tip off the sample, $W_{Adhesion}$ is a measure of attraction between two surfaces).[9, 10] The number of interacting molecules can be calculated from the contact radius at pull off (a_s), for which the (JKR) theory gives:[9, 10]

$$a_s = \left[\frac{3\pi W_{Adhesion} R^2}{2K}\right]^{\frac{1}{3}} \quad (2)$$

Where K is the elastic modulus of the contacting surfaces (64 GPa).[11] Once the contact radius at pull off is known, the contact area at pull off can be calculated.

Here, we have assumed that the polycrystalline Au surface of our AFM tips consists predominantly of (111) facets. From prior studies, it is known that the sulfur atoms of long chain alkanethiols on Au (111) form a commensurate hexagonal (√3×√3) R30 overlayer structure with an S-S spacing of 4.97 Å and a calculated (defect free monolayer) area per molecule of 21.4 $Å^2$. [11, 12] We also note that the areal densities of oligoethylene glycol terminated SAMs have also been estimated to be around 21.4 $Å^2$ per molecule on Au (111) (in the absence of other data, we assume that the oligoethylene glycol terminated SAMs on Au (111) substrate mainly assume a helical

structure).[13] Informed by these previous studies, we have used this value (i.e. 21.4 Å^2 per molecule) as an approximate cross-sectional area for each (EG4) molecule. From the above values, the number of interacting (EG4) molecules (n) between the chemically modified AFM tips and peptide covered samples can be calculated. The mean adhesion force per EG4 molecule can then be easily calculated from the number of interacting molecules using the average mean adhesion force. By using the above-mentioned approach, we have calculated the mean adhesion force per EG4 molecule for (EG4-$C_{14}H_{30}$-CY), (EG4-$C_{14}H_{30}$-CAY), (EG4-$C_{14}H_{30}$-CAT), (EG4-$C_{14}H_{30}$-CAS), (EG4-$C_{14}H_{30}$-CA[p]Y), (EG4-$C_{14}H_{30}$-CA[p]T) and (EG4-$C_{14}H_{30}$-CA[p]S) combinations. The calculated values for these surface (around 180 pN) are higher than the values reported previously for single bond force between hydrogen bonding surfaces in organic solvents (70 pN)[11] (see **Table S2**).

We caution that the calculated mean adhesion force per EG4 molecule is a result of measurements over an ensemble of molecules on the tip, so there is a chance that some EG4 molecules form more than one hydrogen bond with the surface (there are several hydrogen bonding sites present on each EG4 molecule, formation of more than one hydrogen bond per EG4 molecule is possible), we attribute the high value of mean adhesion force per EG4 molecule (around 180 pN) to the possibility of the formation of more than one hydrogen bond per EG4 molecule (i.e. in other words, we believe that some of the EG4 molecules on the tip surface would form more than one hydrogen bond with the peptide-decorated surfaces which would result in higher mean adhesion force per EG4 molecule). We note that, irrespective of the details of the hydrogen bonding between the EG4 molecules and the peptide-decorated surfaces, the value of the mean adhesion force per EG4 molecule is consistent with the formation of at least one hydrogen bond between each EG4 molecule and all of the surfaces investigated here, which provides further

support for the hypothesis that the high adhesion measured between EG4 tips and CY, CAY, CAT, CAS, CA[p]Y, CA[p]T and CA[p]S decorated surfaces under tetradecane is largely due to hydrogen bonding.

Characterizing the Surface Coverage of Peptide-Decorated Surfaces using Cyclic Voltammetry

Table S3 shows the surface coverage, area per molecule and desorption peak potential analysis based on the cyclic voltammograms of peptide monolayers. The surface coverage was calculated using the below equation:

$$Surface\ coverage = \frac{Area\ under\ the\ desorption\ peak}{n_e F} \quad (3)$$

In the above equation, n_e is the number of electrons that are involved in the desorption of a peptide molecule (motivated by previous studies showing that desorption of alkanethiols in basic pH is a one electron process, we have assumed that $n_e=1$[14, 15]) and F (Faraday constant) is the magnitude of electric charge per mole of electrons (F≈ 96 485 (A.s)/mol).[14, 15, 16] We note that the calculated area per molecule for all of the peptides lies between 3.1 and 4.5 $Å^2$ which is interestingly lower than the area per molecule calculated previously for alkanethiols 21.4 $Å^2$.[11, 12] This observation strongly implies that the desorption of the peptide monolayers in alkaline solution is a multielectron process and is a fundamentally different process than the desorption of alkanethiols in basic conditions (for which $n_e=1$[14, 15]). We note that this is not surprising, since for example desorption of alkanethiols in acidic conditions is shown to be multielectron process ($n_e≈3$; the exact mechanism for this desorption process is not fully understood yet).[14, 15] We would like to mention that our key conclusions in the manuscript is completely independent of this

observation (see below; elucidating the desorption mechanism of peptide monolayers from gold films is beyond the scope of this study).

We would like to end this section by pointing out that in our calculations we used geometric surface area in calculating surface coverages and we acknowledge that the actual surface area of gold electrodes is expected to be higher than the geometric surface area because of surface roughness (the actual surface area of polycrystalline gold films prepared under similar conditions to this study is reported to be 1.1 to 1.2 times larger than the geometric surface area of the films[14, 15]). We would like to mention that our conclusion that the desorption of the peptide monolayers in alkaline solution is a multielectron process is independent of the roughness. More specifically, we recalculated the area per molecule assuming a relatively rough gold electrode (i.e. actual surface area=1.2 geometric surface area) and found that the area per molecule for all of the peptides lies between 3.7 and 5.4 $Å^2$ which is still lower than the area per molecule calculated previously for alkanethiols 21.4 $Å^2$ (see **Table S3** for more details).

Calculating the Faradaic Energy Associated with the Shifts in Desorption Peak Potentials of Peptides (CT vs CV and CS vs CA)

As mentioned in the manuscript, the complexity of electrochemical desorption of monolayers does not allow the direct estimation of the differences in the strength of intra-monolayer interactions of dipeptide monolayers from the shifts in desorption peak potentials (CT compared with CV and CS compared to CA).[14, 15] For example, monolayers of alkanethiols with longer chain lengths desorb at more negative potentials which has been attributed to the stronger intra-monolayer van der Waals interactions in monolayers of alkanethiols with longer chain

lengths.[14, 15] It has been shown that the desorption peak potential of monolayers of alkanethiols is linearly correlated with the length of alkyl chain with the slope of -15 mV/CH_2.[14, 15] This shift in the desorption peak potential can be used to calculate a Faradaic stabilization energy using the below equation :[14, 15, 16]

$$Faradaic\ stabilization\ energy = -n_e F(shift\ in\ the\ desorption\ peak\ potential) \quad (4)$$

In the above equation, n_e is the number of electrons that are involved in the desorption of a molecule (n_e=1 for alkanethiols desorption in basic pH[14, 15]) and F (Faraday constant) is the magnitude of electric charge per mole of electrons (F≈ 96 485 (A.s)/mol).[14, 15, 16] Using equation (4), one calculates a value of 1.4 (kJ/mol)/CH_2 for Faradaic stabilization energy.[14, 15, 16] We note that the interaction energy between alkyl chains has been estimated experimentally (by measuring the heat of desorption of aliphatic alcohol monolayers from platinum[17] and silver[18] surfaces) and theoretically (using a hybrid density functional (DFT) and Møller–Plesset perturbation theory (MP2)) to be 4±1 (kJ/mol)/CH_2.[19] Although, Faradaic stabilization energy clearly underestimates the interaction energy between alkyl chains, its order of magnitude is comparable to that of the interaction energy between alkyl chains.[14, 15, 17, 18, 19]

Using the values presented in **Table 3** of the manuscript, we calculated the Faradaic stabilization energy corresponding to the shifts in desorption peak potentials (CT compared with CV and CS compared to CA) to be 1.4±0.3 kJ/mol and 0.9±0.5 kJ/mol respectively (assuming n_e=1). We would like to mention that the strength of most hydrogen bonds lie between 5 and 40 kJ/mol[20, 21] and that the observed shifts in desorption peak potentials (CT compared with CV and CS compared to CA) is in qualitative agreement with a strength of a hydrogen bond.

We note that the above conclusion is independent of exact value of n_e. Although our surface coverage calculations strongly imply that $n_e \geq 1$, assuming higher values of n_e will increase the

calculated values of the Faradaic stabilization energy and further reinforces our conclusion that the observed shifts in desorption peak potentials (CT compared with CV and CS compared to CA) is in qualitative agreement with a strength of a hydrogen bond.

We would like to finish this section by commenting on the ionization sate of -OH group of tyrosine, serine and threonine. The -OH group of serine and threonine are practically non-ionizable (pK_a>13)[22], while the pK_a value of -OH group of tyrosine is reported to be ~10[22]. We have performed all of CV measurements at pH=8.5 and therefore we expect the -OH group of tyrosine, serine and threonine to be mostly non-ionized and being able of forming hydrogen bonds.

Characterizing the Phosphopeptide-Decorated Surfaces using Cyclic Voltammetry

Cyclic voltammograms (after baseline correction) for the reductive desorption from C[p]Y, CF, C[p]T, CV, C[p]S, CA, CA[p]Y, CAF, CA[p]T, CAV, CA[p]S and CAA-decorated surfaces are shown in **Figure S12A, S12B, S12C, S12D, S12E and S12F**. Interestingly, we do not observe any meaningful difference (within experimental uncertainty) in the electrochemical stability as a result of addition of phosphate group to the peptide structure (see **Table S4** for detailed comparison). These experiments do not provide any evidence for the existence of intra-monolayer hydrogen bonding of the phosphate group.

We would like to mention that the phosphate group of phosphorylated tyrosine, phosphorylated serine or phosphorylated threonine has either one or two -OH groups.[23, 24, 25] The pK_a of the first -OH group is ~2 and the pK_a of the second -OH group is ~6.[23, 24, 25] At physiological pH (and also the pH at which we prepared phosphorylated peptide decorated surfaces

for LC measurements), the phosphate group is expected to have only one -OH group.[23, 24, 25] Unfortunately, the lowest pH at which we could perform the cyclic voltammetry measurements without significant disturbance due to hydrogen evolution at the working electrode was 8.5 (the small fluctuations observed in some cyclic voltammograms between -1.1 V and -1.2 V are due to hydrogen evolution at the working electrode; see **Figure 12**). Also, we note that, in principle, performing cyclic voltammetry measurements in acid environments (pH<7) cannot be used to compare the stability of monolayers, since it has been shown that the gold atoms also desorb in acidic environment which makes the interpretation of the shifts in desorption peaks meaningless.[14, 15] Overall, although our cyclic voltammetry measurements did not provide any evidence for the intra-monolayer hydrogen bonding in phosphorylated peptide-decorated monolayers, we cannot rule out intra-monolayer hydrogen bonding in phosphorylated peptide-decorated monolayers based on these measurements only (i.e. at pH=8.5, it is likely that most of the -OH groups are already ionized and not available for hydrogen bonding).

Tables

Table S1. Peak assignments of dipeptides and tripeptide monolayers using PM-IRRAS.

Position (cm^{-1})	Molecule	Assignment
~1259	All	Methyl rocking & C-C stretching[26]
~1512 to ~1518	CY, CAY, C[p]Y and CA[p]Y	C=C[27, 28]
~1539	All	N-C=O (Amide II)[29, 30]
~1684	All	C=O (amide I)[29, 30]

Table S2. Number of interacting molecules (n) and mean adhesion force per EG4 molecule (pN) calculated based on (JKR) theory of adhesion mechanics

Tip-Solvent-Substrate Combination	Number of interacting molecules (n)	Mean adhesion force per EG4 Molecule (pN)
(EG4-$C_{14}H_{30}$-CY)	57	174
(EG4-$C_{14}H_{30}$-CAY)	60	176
(EG4-$C_{14}H_{30}$-CAT)	58	173
(EG4-$C_{14}H_{30}$-CAS)	73	196
(EG4-$C_{14}H_{30}$-CA[p]Y)	56	171
(EG4-$C_{14}H_{30}$-CA[p]T)	62	180
(EG4-$C_{14}H_{30}$-CA[p]S)	57	174

Table S3. Surface coverage, area per molecule and desorption peak potential analysis based on the cyclic voltammograms of peptide monolayers (the numbers presented in parentheses in the third column are calculated assuming a rough gold electrode (i.e. actual surface area=1.2 geometric surface area)).

Surface specification	Surface coverage (molecules/cm^2)	Area per molecule (Å^2/molecule)	Desorption peak potential (V)
CY monolayer	$(2.4\pm0.3) \times 10^{15}$	4.4±0.5 (5.3±0.6)	-0.839±0.003
C[p]Y monolayer	$(2.3\pm0.3) \times 10^{15}$	4.4±0.5 (5.3±0.6)	-0.839±0.002
CF monolayer	$(2.2\pm0.2) \times 10^{15}$	4.5±0.3 (5.4±0.4)	-0.841±0.002
CT monolayer	$(2.8\pm0.1) \times 10^{15}$	3.6±0.1 (4.4±0.2)	-0.841±0.001
C[p]T monolayer	$(3.1\pm0.2) \times 10^{15}$	3.4±0.3 (4.1±0.3)	-0.831±0.003
CV monolayer	$(3.0\pm0.2) \times 10^{15}$	3.3±0.2 (4.0±0.2)	-0.826±0.002
CS monolayer	$(2.7\pm0.2) \times 10^{15}$	3.8±0.3 (4.5±0.3)	-0.841±0.001
C[p]S monolayer	$(3.1\pm0.3) \times 10^{15}$	3.4±0.34 (4.1±0.4)	-0.837±0.003
CA monolayer	$(3.0\pm0.3) \times 10^{15}$	3.5±0.4 (4.2±0.5)	-0.831±0.004
CAY monolayer	$(2.5\pm0.3) \times 10^{15}$	4.1±0.4 (4.9±0.5)	-0.841±0.001
CA[p]Y monolayer	$(2.5\pm0.2) \times 10^{15}$	4.1±0.3 (4.9±0.4)	-0.839±0.002
CAF monolayer	$(2.4\pm0.1) \times 10^{15}$	4.2±0.2 (5.1±0.2)	-0.841±0.002
CAT monolayer	$(3.1\pm0.2) \times 10^{15}$	3.4±0.3 (4.1±0.3)	-0.837±0.001
CA[p]T monolayer	$(2.7\pm0.2) \times 10^{15}$	3.8±0.3 (4.6±0.3)	-0.841±0.002

CAV monolayer	$(2.7\pm0.1) \times 10^{15}$	3.8±0.2 (4.6±0.2)	-0.839±0.001
CAS monolayer	$(3.0\pm0.1) \times 10^{15}$	3.3±0.2 (4.0±0.2)	-0.841±0.001
CA[p]S monolayer	$(3.1\pm0.2) \times 10^{15}$	3.4±0.3 (4.1±0.3)	-0.841±0.002
CAA monolayer	$(3.3\pm0.1) \times 10^{15}$	3.1±0.1 (3.7±0.1)	-0.840±0.003

Table S4. Analysis of shifts in desorption peak potentials (E_{peak})

Amino Acid	**(Epeak (CX)- Epeak (CX*)) (mV)**	**(Epeak (CAX)- Epeak (CAX*)) (mV)**
X=[p]Y and X*=F	2±4	2±4
X=[p]T and X*=V	-5±5	-2±3
X=[p]S and X*=A	-6±7	-1±5

Figures

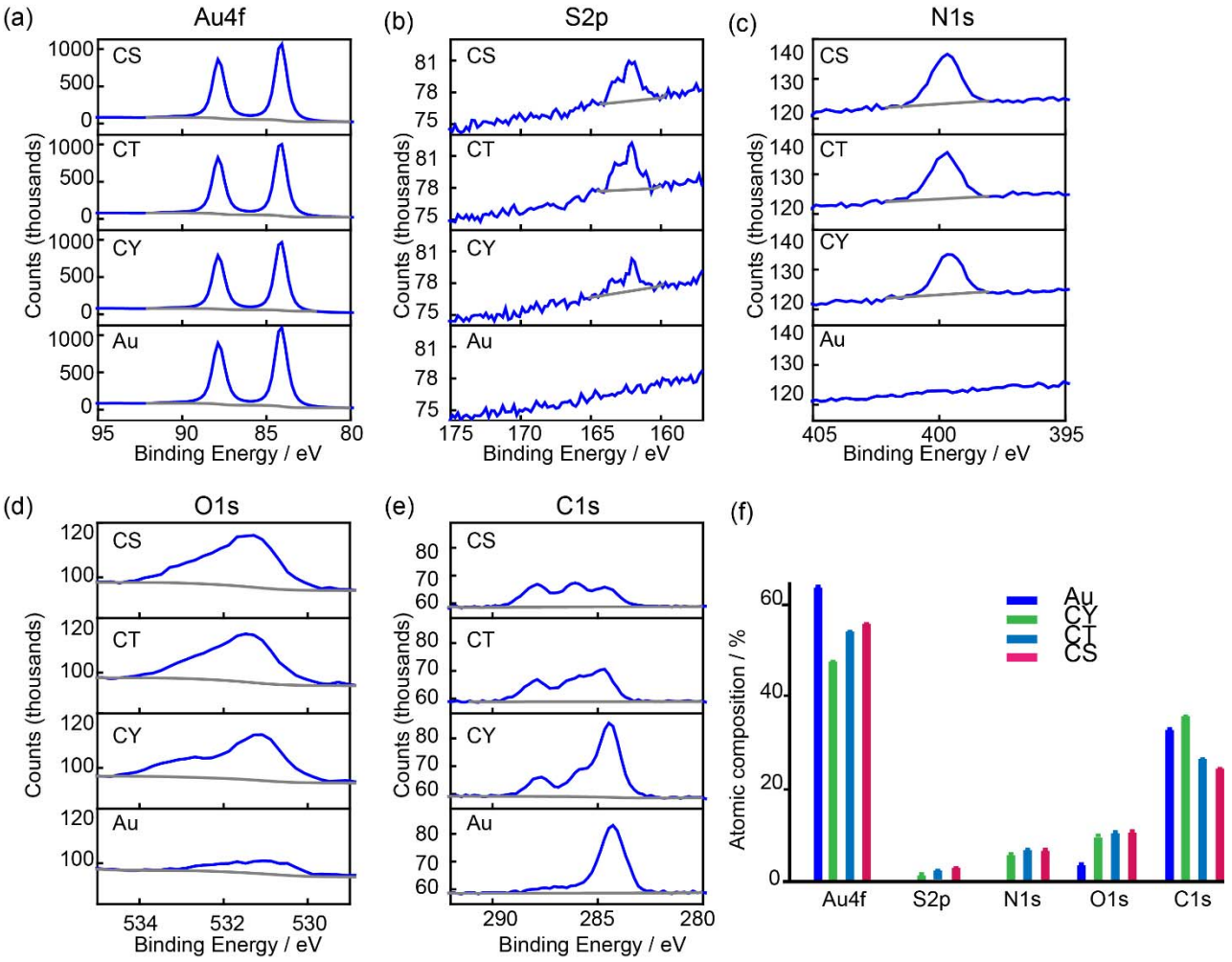

Figure S1. XPS spectra of dipeptide monolayers formed on Au surfaces (A) Au (4f) peak (B) S (2p) peak (C) N (1s) peak (D) O (1s) peak (E) C (1s) peak (F) Calculated atomic compositions.

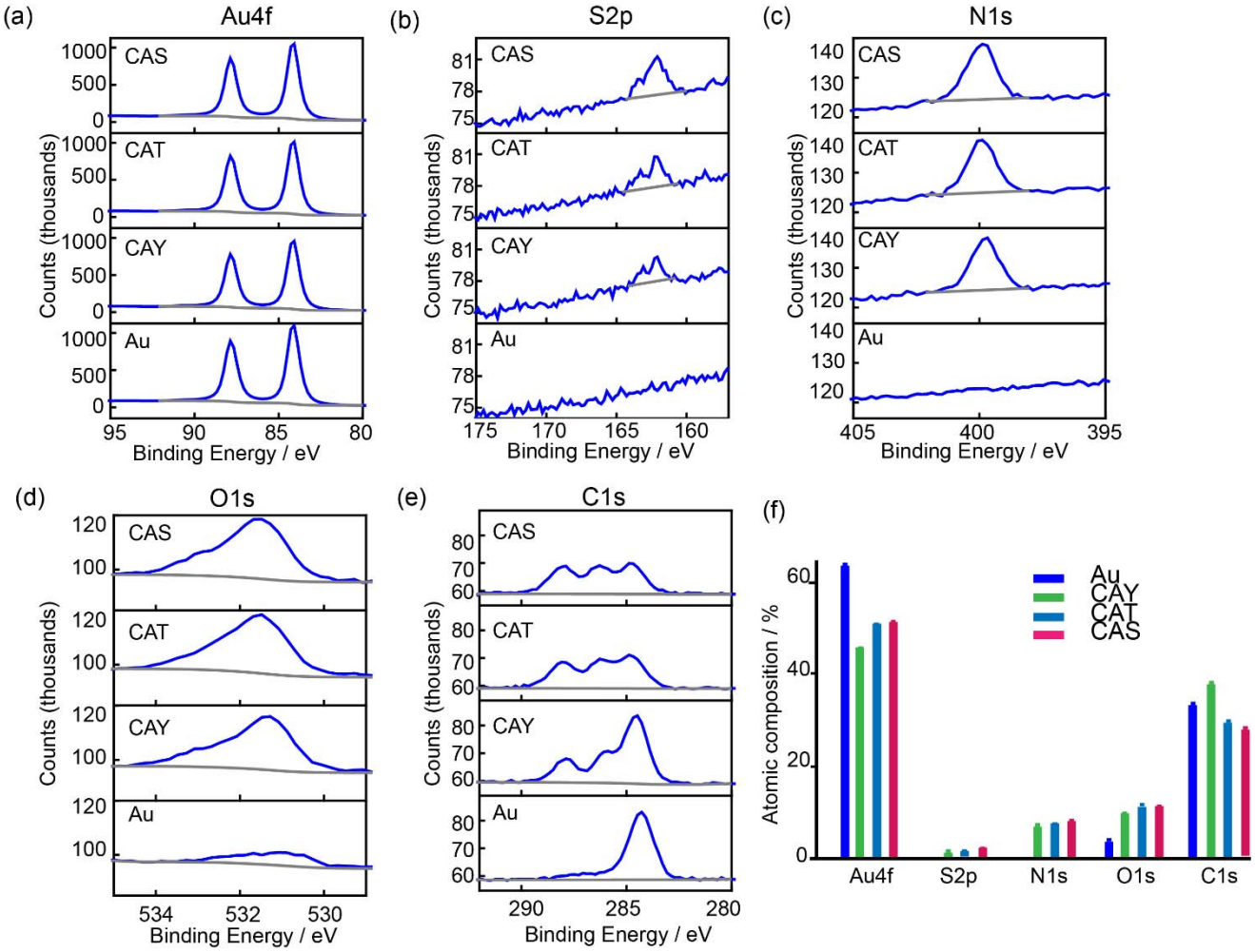

Figure S2. XPS spectra of tripeptide monolayers formed on Au surfaces (A) Au (4f) peak (B) S (2p) peak (C) N (1s) peak (D) O (1s) peak (E) C (1s) peak (F) Calculated atomic compositions.

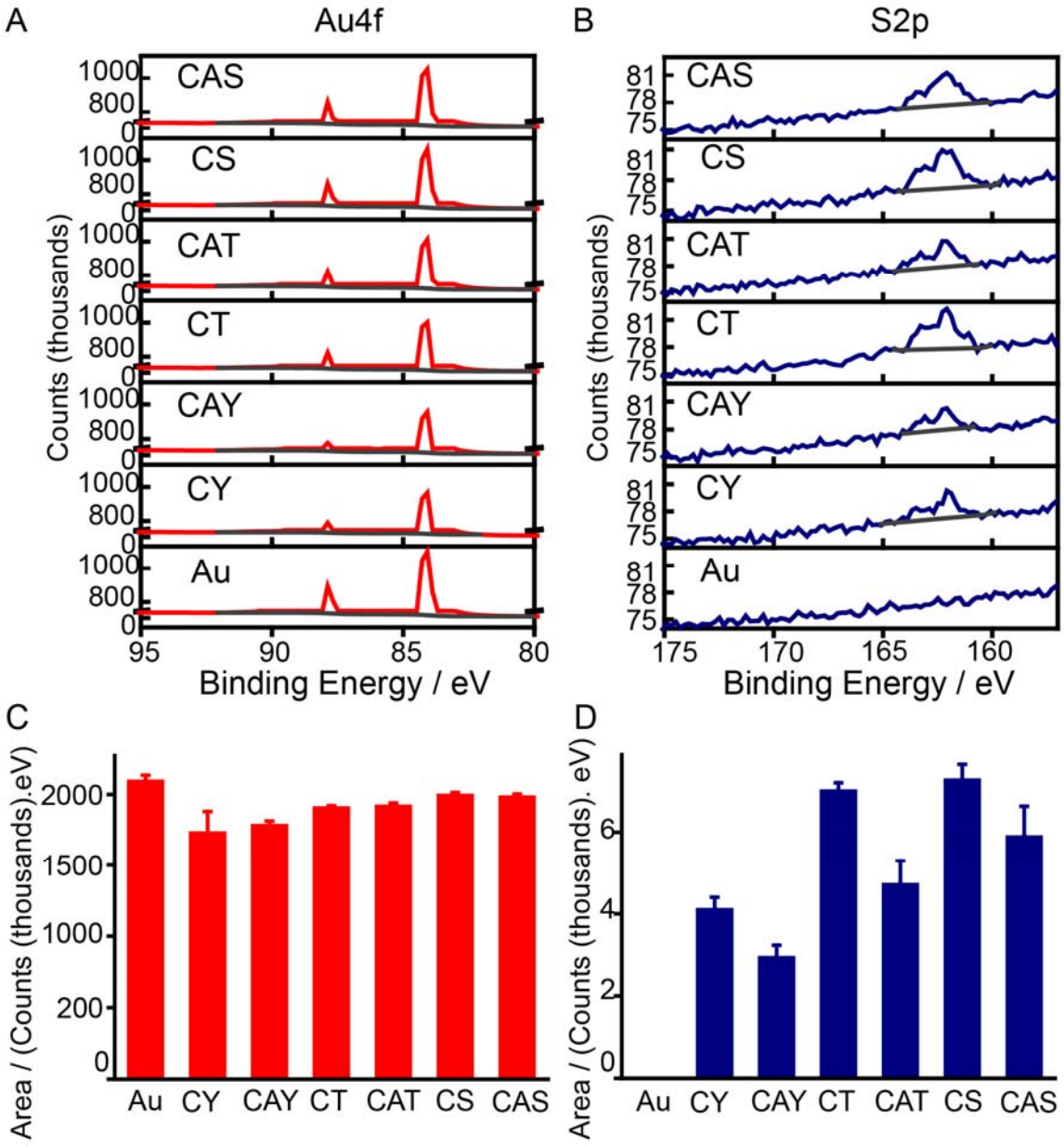

Figure S3. XPS spectra of non-phosphorylated dipeptide and tripeptide monolayers formed on Au surfaces (A) Au (4f) peak (B) S (2p) peak (C) Calculated Au 4f peak areas (D) Calculated S (2p) peak areas.

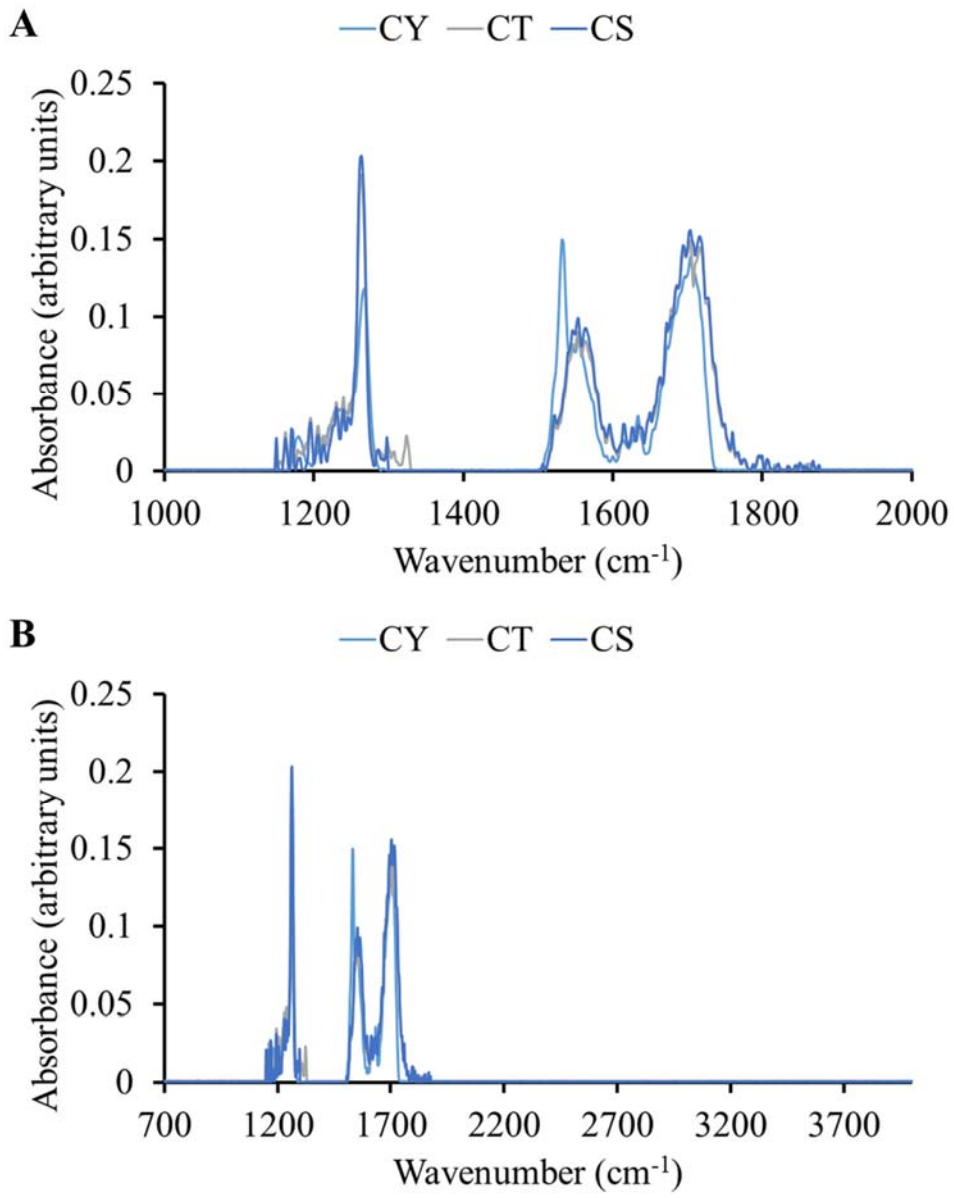

Figure S4. (A) PM-IRRAS spectra of CY, CT and CS monolayers formed on Au surfaces (the spectra are shown in the range of 1000 cm^{-1} to 2000 cm^{-1}) (B) (A) PM-IRRAS spectra of CY, CT and CS monolayers formed on Au surfaces (the spectra are shown in the range of 700 cm^{-1} to 4000 cm^{-1}).

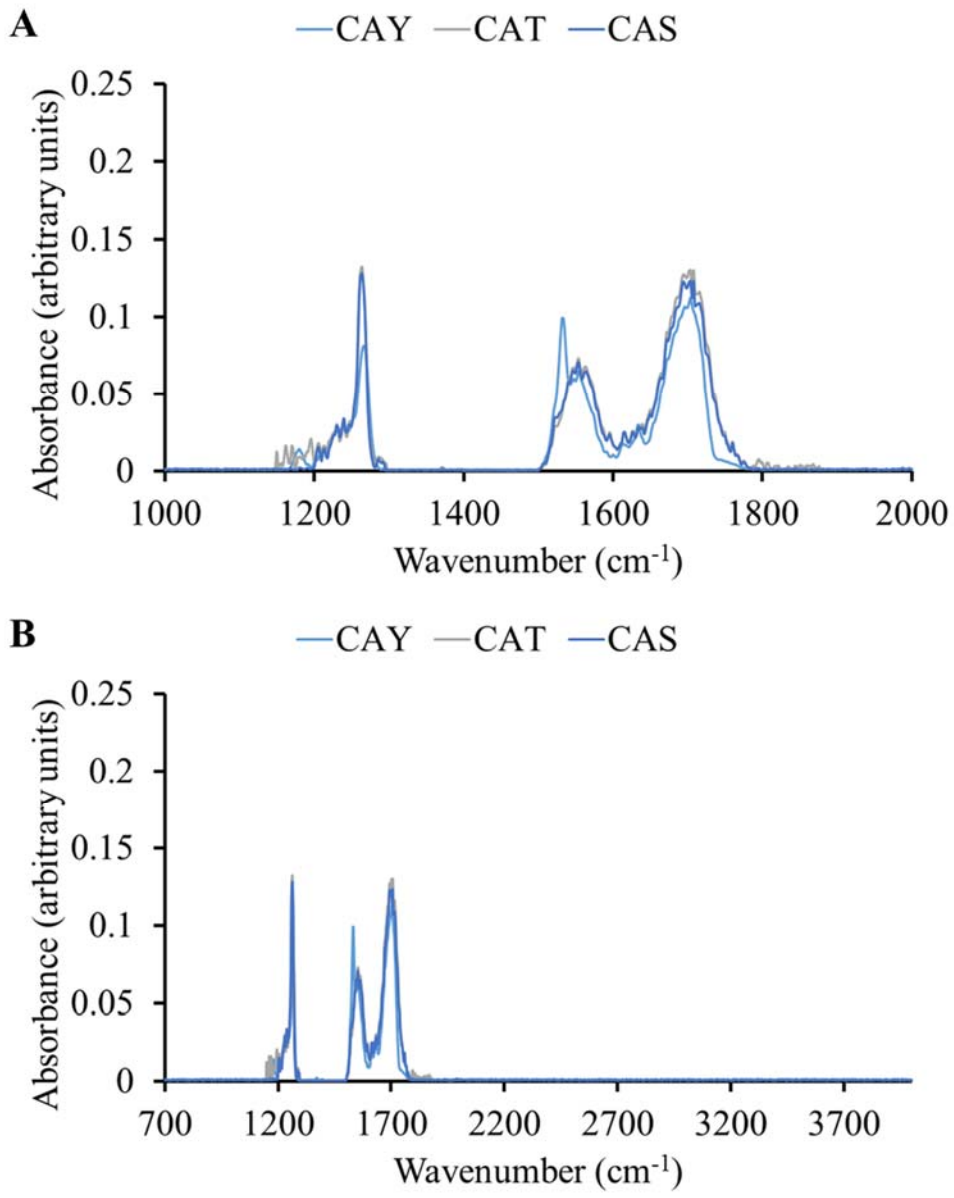

Figure S5. (A) PM-IRRAS spectra of CAY, CAT and CAS monolayers formed on Au surfaces (the spectra are shown in the range of 1000 cm^{-1} to 2000 cm^{-1}) (B) (A) PM-IRRAS spectra of CAY, CAT and CAS monolayers formed on Au surfaces (the spectra are shown in the range of 700 cm^{-1} to 4000 cm^{-1}).

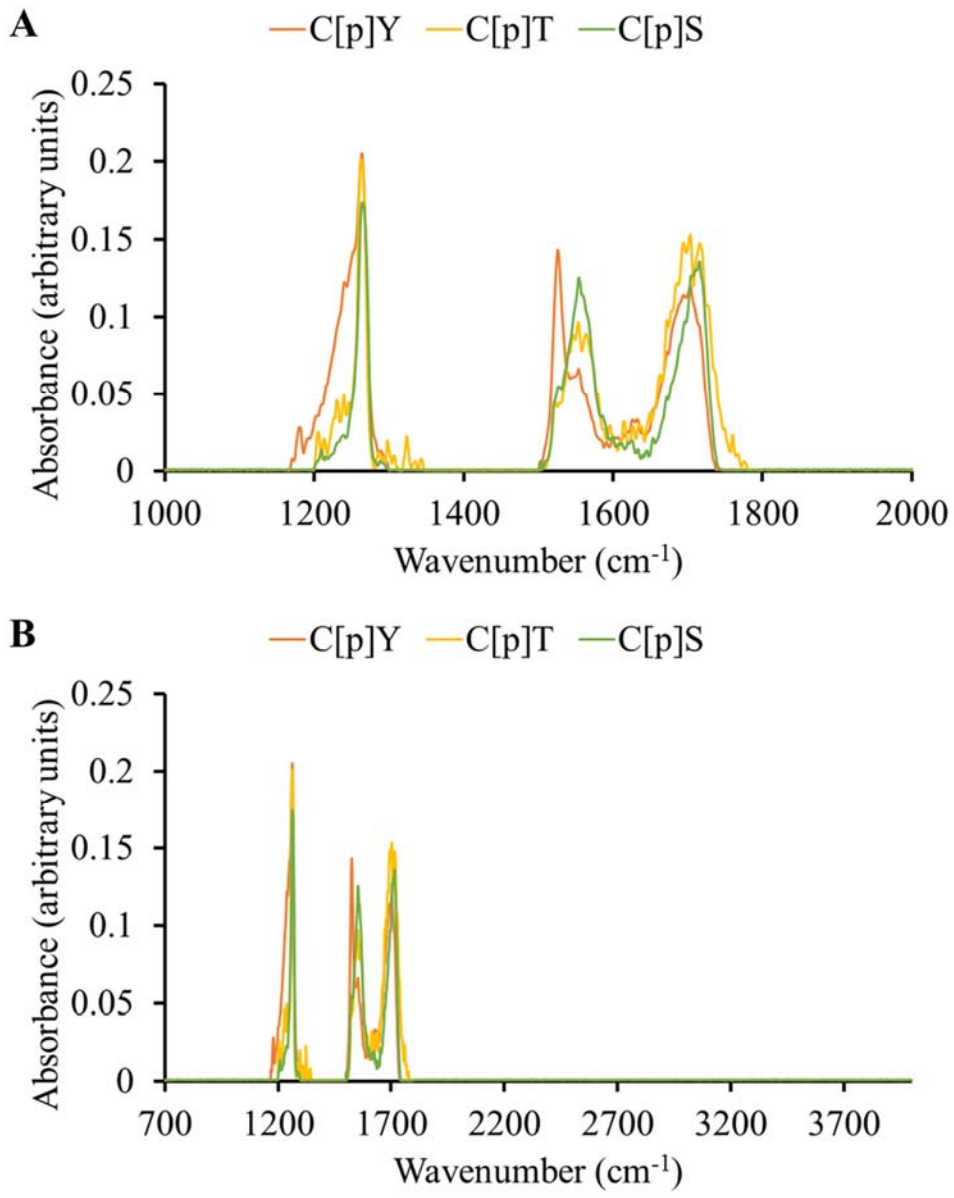

Figure S6. (A) PM-IRRAS spectra of C[p]Y, C[p]T and C[p]S monolayers formed on Au surfaces (the spectra are shown in the range of 1000 cm^{-1} to 2000 cm^{-1}) (B) (A) PM-IRRAS spectra of C[p]Y, C[p]T and C[p]S monolayers formed on Au surfaces (the spectra are shown in the range of 700 cm^{-1} to 4000 cm^{-1}).

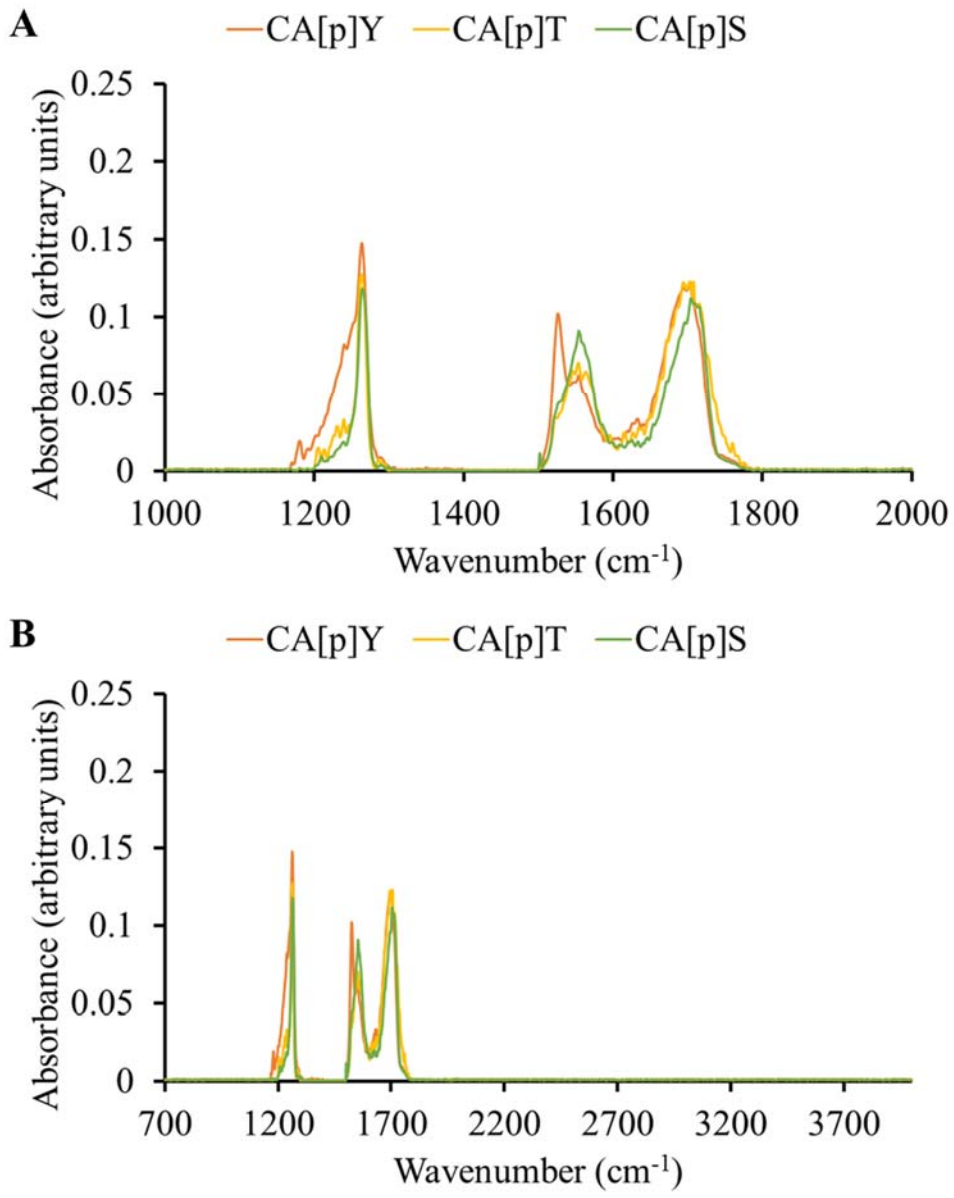

Figure S7. (A) PM-IRRAS spectra of CA[p]Y, CA[p]T and CA[p]S monolayers formed on Au surfaces (the spectra are shown in the range of 1000 cm^{-1} to 2000 cm^{-1}) (B) (A) PM-IRRAS spectra of CA[p]Y, CA[p]T and CA[p]S monolayers formed on Au surfaces (the spectra are shown in the range of 700 cm^{-1} to 4000 cm^{-1}).

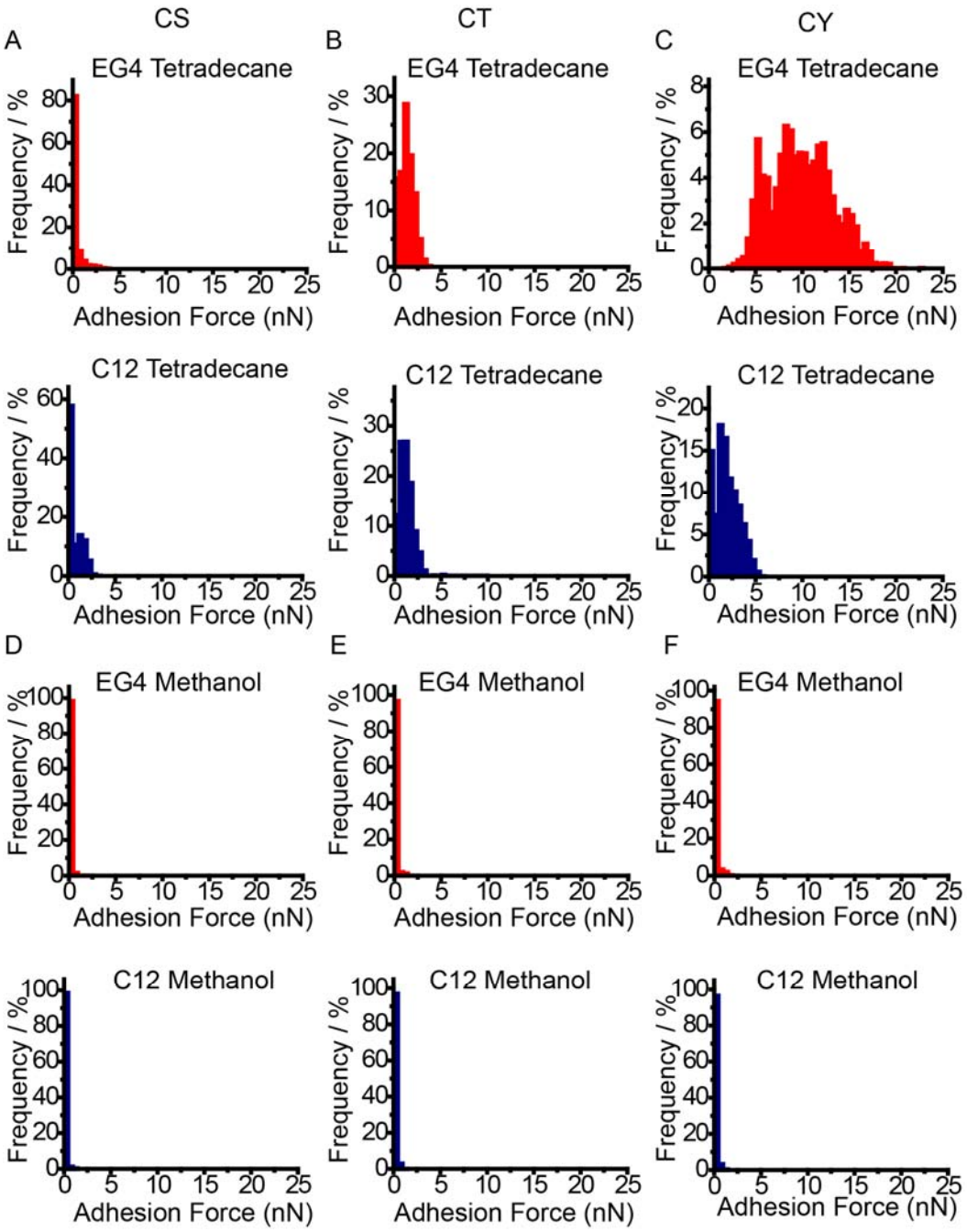

Figure S8. Adhesion force histograms obtained by using EG4 modified tips (red bar) and $C_{12}SH$ modified tips (blue bar) on non-phosphorylated dipeptide-decorated surfaces. (A) CS in

tetradecane (B) CT in tetradecane (C) CY in tetradecane (D) CS in methanol (E) CT in methanol (F) CY in methanol.

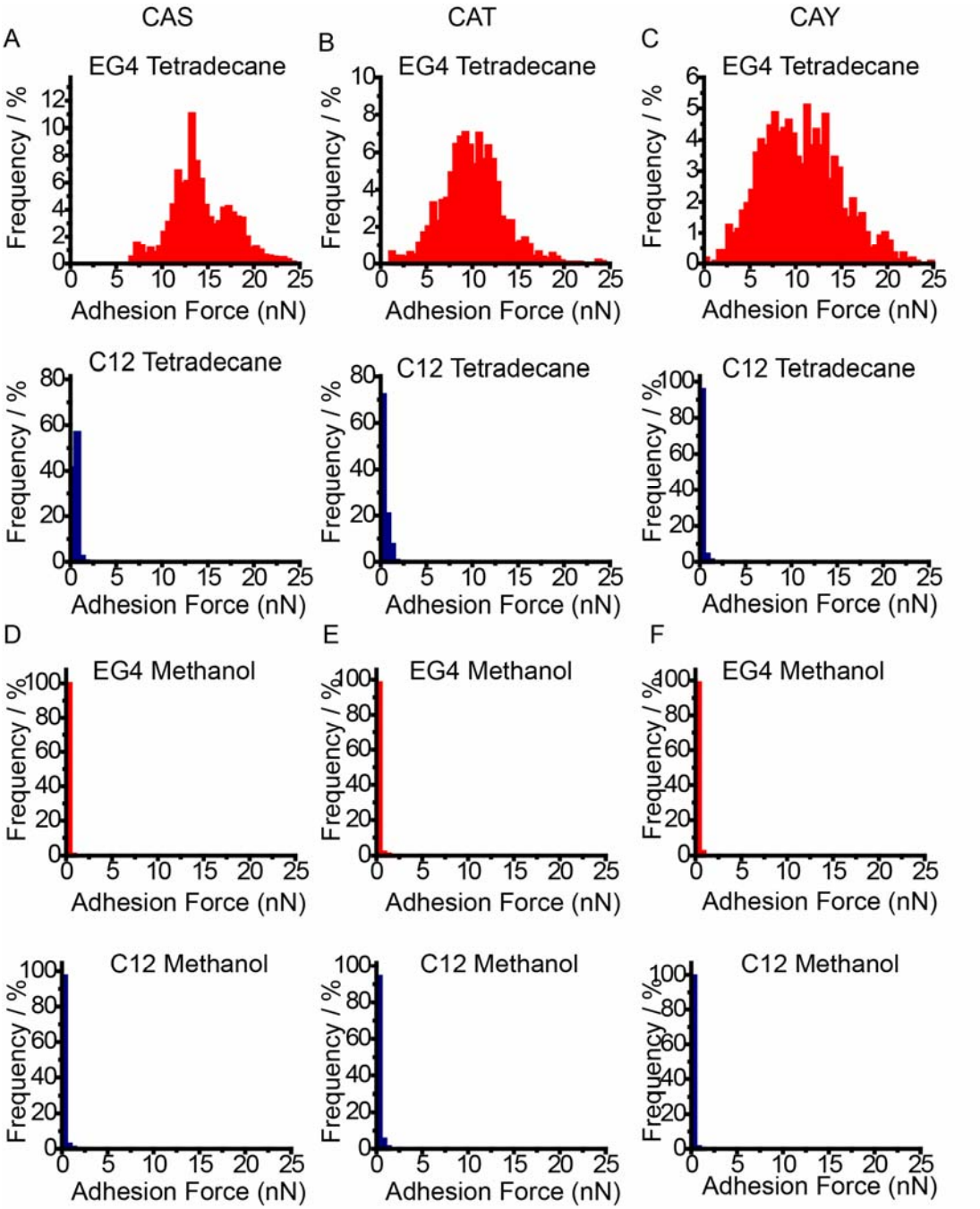

Figure S9. Adhesion force histograms obtained by using EG4 modified tips (red bar) and $C_{12}SH$ modified tips (blue bar) on non-phosphorylated tripeptide-decorated surfaces. (A) CAS in tetradecane (B) CAT in tetradecane (C) CAY in tetradecane (D) CAS in methanol (E) CAT in methanol (F) CAY in methanol.

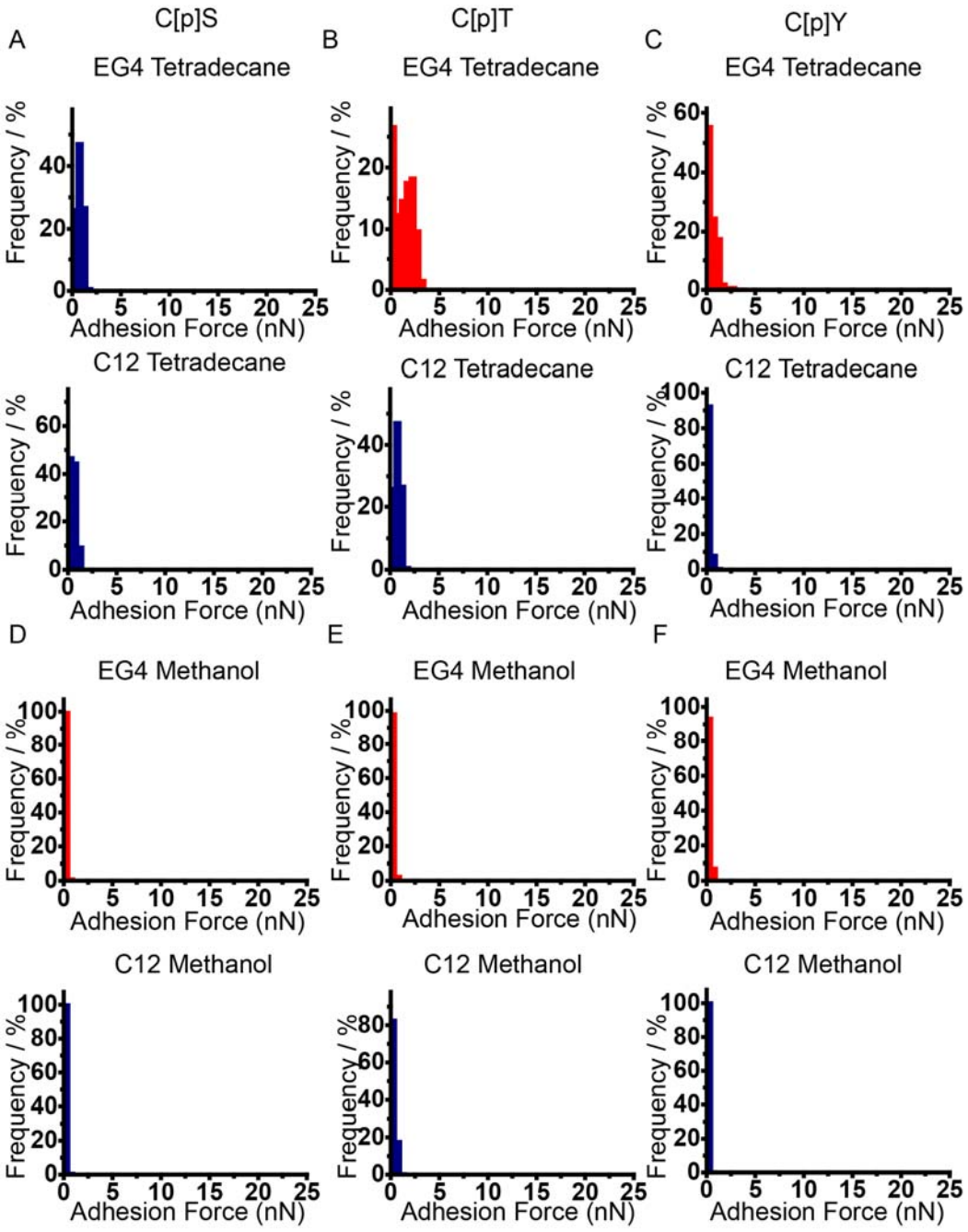

Figure S10. Adhesion force histograms obtained by using EG4 modified tips (red bar) and $C_{12}SH$ modified tips (blue bar) on phosphorylated dipeptide-decorated surfaces. (A) C[p]S in tetradecane (B) C[p]T in tetradecane (C) C[p]Y in tetradecane (D) C[p]S in methanol (E) C[p]T in methanol (F) C[p]Y in methanol.

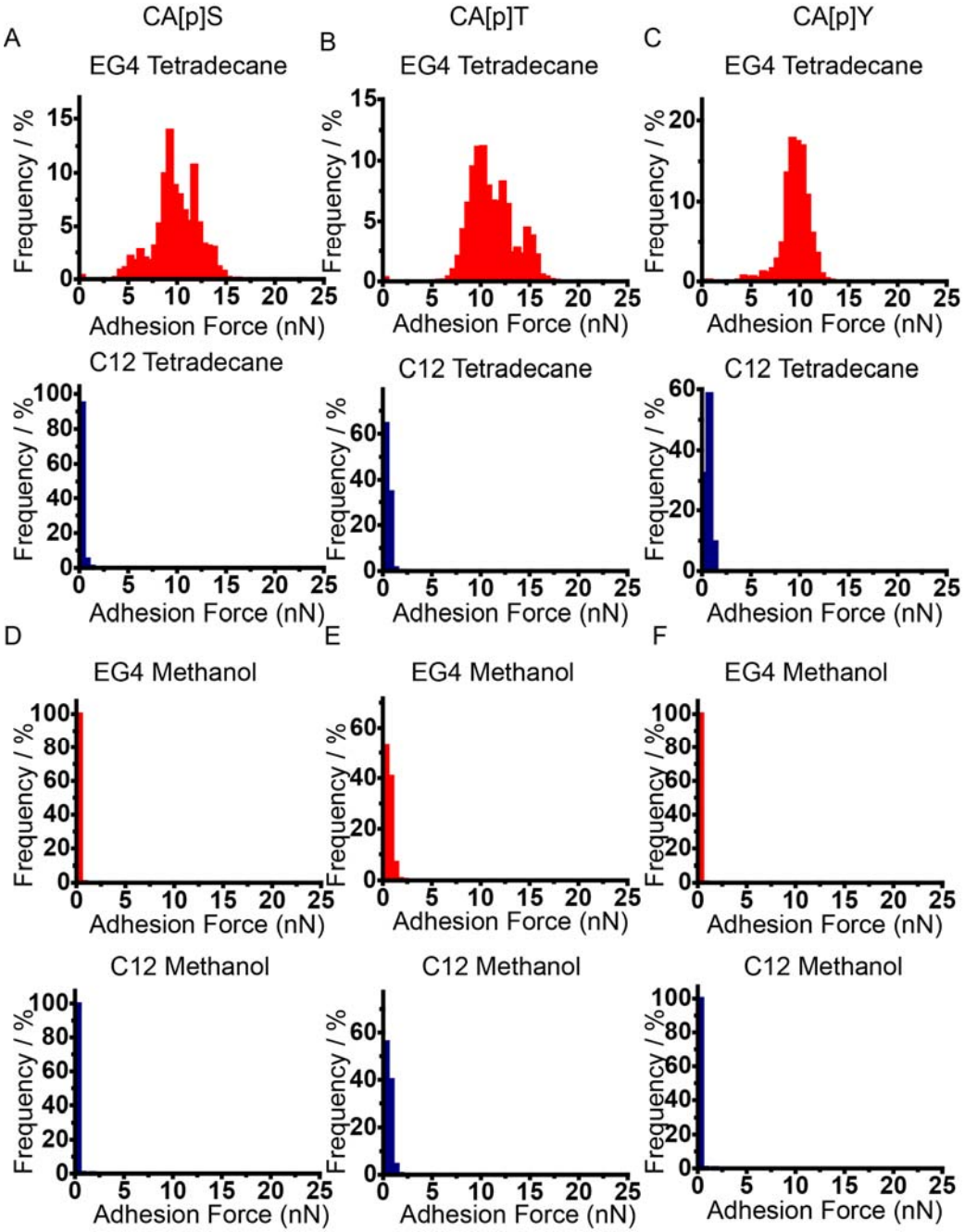

Figure S11. Adhesion force histograms obtained by using EG4 modified tips (red bar) and $C_{12}SH$ modified tips (blue bar) on phosphorylated tripeptide-decorated surfaces. (A) CA[p]S in tetradecane (B) CA[p]T in tetradecane (C) CA[p]Y in tetradecane (D) CA[p]S in methanol (E) CA[p]T in methanol (F) CA[p]Y in methanol.

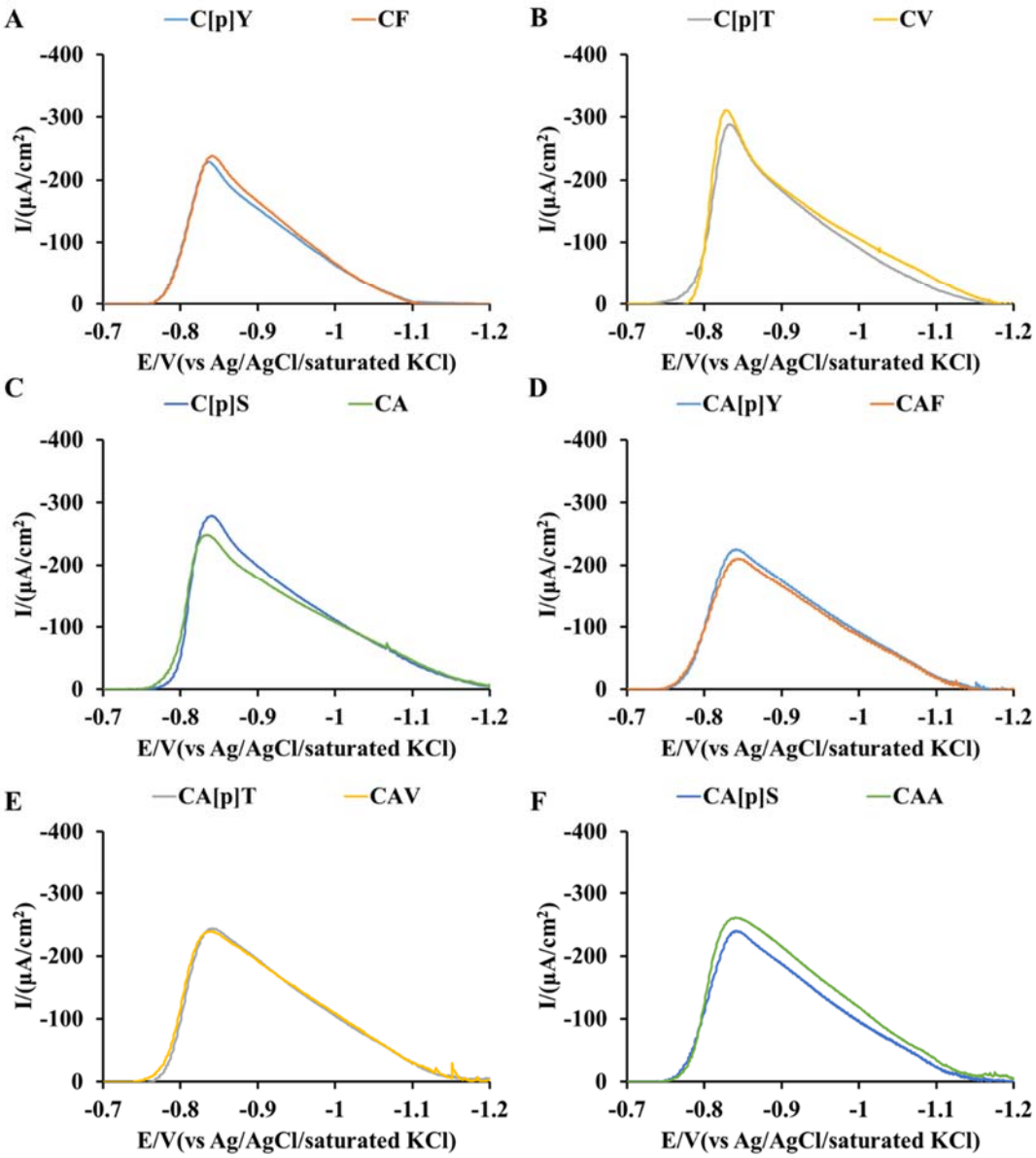

Figure S12. Cyclic voltammograms for the reductive desorption from dipeptide and tripeptide decorated surfaces: (A) C[p]Y and CF-decorated surfaces (B) C[p]T and CV-decorated surfaces

(C) C[p]S and CA-decorated surfaces (D) CA[p]Y and CAF-decorated surfaces (E) CA[p]T and CAV-decorated surfaces (F) CA[p]S and CAA-decorated surfaces (cyclic voltammograms were recorded in 0.5 M KCl solution (the solution pH was adjusted to be 8.5 using KOH; scan rate: 100 mV/s)).

References

1. Bai, Y.; Abbott, N. L. Enantiomeric Interactions between Liquid Crystals and Organized Monolayers of Tyrosine-Containing Dipeptides. *Journal of the American Chemical Society* **2012,** *134* (1), 548-558.
2. Luk, Y. Y.; Tingey, M. L.; Dickson, K. A.; Raines, R. T.; Abbott, N. L. Imaging the Binding Ability of Proteins Immobilized on Surfaces with Different Orientations by using Liquid Crystals. *J. Am. Chem. Soc.* **2004,** *126* (29), 9024-9032.
3. Bai, Y.; Abbasi, R.; Wang, C.; Abbott, N. L. Liquid Crystals Anchored on Mixed Monolayers of Chiral versus Achiral Molecules: Continuous Change in Orientation as a Function of Enantiomeric Excess. *Angewandte Chemie International Edition* **2014,** *53* (31), 8079-8083.
4. Rosu, D. M.; Jones, J. C.; Hsu, J. W. P.; Kavanagh, K. L.; Tsankov, D.; Schade, U.; Esser, N.; Hinrichs, K. Molecular Orientation in Octanedithiol and Hexadecanethiol Monolayers on GaAs and Au Measured by Infrared Spectroscopic Ellipsometry. *Langmuir* **2008,** *25* (2), 919-923.
5. Acevedo-Vélez, C.; Andre, G.; Dufrêne, Y. F.; Gellman, S. H.; Abbott, N. L. Single-Molecule Force Spectroscopy of β-Peptides That Display Well-Defined Three-Dimensional Chemical Patterns. *Journal of the American Chemical Society* **2011,** *133* (11), 3981-3988.
6. Hinterdorfer, P.; Dufrene, Y. F. Detection and Localization of Single Molecular Recognition Events using Atomic Force Microscopy. *Nat Meth* **2006,** *3* (5), 347-355.
7. Pan, S.; Castner, D. G.; Ratner, B. D. Multitechnique Surface Characterization of Derivatization Efficiencies for Hydroxyl-terminated Self-assembled Monolayers. *Langmuir* **1998,** *14* (13), 3545-3550.
8. Smith, B. C. *Infrared Spectral Interpretation: A systematic Approach*; CRC press: New York, 1998.
9. Johnson, K.; Kendall, K.; Roberts, A. In *Surface Energy and the Contact of Elastic Solids*, Proceedings of the Royal Society of London A: Mathematical, Physical and Engineering Sciences, 1971; The Royal Society, pp 301-313.
10. Hiemenz, P. C.; Rajagopalan, R. *Principles of Colloid and Surface Chemistry, Revised and Expanded*; CRC press1997; Vol. 14.
11. Papastavrou, G.; Akari, S. Interaction Forces between OH-groups in Different Solvents as Observed by Scanning Force Microscopy. *Colloids and Surfaces A: Physicochemical and Engineering Aspects* **2000,** *164* (2–3), 175-181.
12. Porter, M. D.; Bright, T. B.; Allara, D. L.; Chidsey, C. E. D. Spontaneously Organized Molecular Assemblies. 4. Structural Characterization of n-alkyl Thiol Monolayers on Gold by Optical Ellipsometry, Infrared Spectroscopy, and Electrochemistry. *Journal of the American Chemical Society* **1987,** *109* (12), 3559-3568.

13. Harder, P.; Grunze, M.; Dahint, R.; Whitesides, G. M.; Laibinis, P. E. Molecular Conformation in Oligo(ethylene glycol)-Terminated Self-Assembled Monolayers on Gold and Silver Surfaces Determines Their Ability To Resist Protein Adsorption. *The Journal of Physical Chemistry B* **1998,** *102* (2), 426-436.
14. Luo, M.; Frechette, J. Electrochemical Stability of Low-density Carboxylic Acid Terminated Monolayers. *The Journal of Physical Chemistry C* **2010,** *114* (47), 20167-20172.
15. Widrig, C. A.; Chung, C.; Porter, M. D. The Electrochemical Desorption of n-alkanethiol Monolayers from Polycrystalline Au and Ag Electrodes. *Journal of Electroanalytical Chemistry and Interfacial Electrochemistry* **1991,** *310* (1), 335-359.
16. Pletcher, D. *A First Course in Electrode Processes*; Royal Society of Chemistry: Cambridge, United Kingdom, 2009.
17. Sexton, B. A.; Rendulic, K. D.; Huges, A. E. Decomposition Pathways of C1-C4 Alcohols Adsorbed on Platinum (111). *Surface Science* **1982,** *121* (1), 181-198.
18. Zhang, R.; Gellman, A. J. Straight-chain Alcohol Adsorption on the Ag (110) Surface. *Journal of Physical Chemistry;(United States)* **1991,** *95* (19).
19. Torres, E.; Blumenau, A. T.; Biedermann, P. U. Steric and Chain Length Effects in the Structures of Alkanethiol Self‐Assembled Monolayers on Au (111). *ChemPhysChem* **2011,** *12* (5), 999-1009.
20. Israelachvili, J. N. *Intermolecular and Surface Forces*; Academic press: New York, 2011.
21. Prausnitz, J. M.; Lichtenthaler, R. N.; de Azevedo, E. G. *Molecular Thermodynamics of Fluid-phase Equilibria*; Pearson Education: Upper Saddle River, New Jersey, 1998.
22. Nelson, D. L. *Lehninger Principles of Biochemistry*; 6th ed.; W. H. Freeman and Co.: New york, NY, 2012.
23. Hoffmann, R.; Reichert, I.; Wachs, W. O.; Zeppezauer, M.; Kalbitzer, H. R. 1H and 31P NMR Spectroscopy of Phosphorylated Model Peptides. *International Journal of Peptide and Protein Research* **1994,** *44* (3), 193-198.
24. Śmiechowski, M. Theoretical pKa Prediction of O-phosphoserine in Aqueous Solution. *Chemical Physics Letters* **2010,** *501* (1–3), 123-129.
25. Wojciechowski, M.; Grycuk, T.; Antosiewicz, J. M.; Lesyng, B. Prediction of Secondary Ionization of the Phosphate Group in Phosphotyrosine Peptides. *Biophysical Journal 84* (2), 750-756.
26. Hostetler, M. J.; Stokes, J. J.; Murray, R. W. Infrared Spectroscopy of Three-dimensional Self-assembled Monolayers: N-alkanethiolate Monolayers on Gold Cluster Compounds. *Langmuir* **1996,** *12* (15), 3604-3612.
27. Hernández, B.; Pflüger, F.; Adenier, A.; Kruglik, S. G.; Ghomi, M. Vibrational Analysis of Amino Acids and Short Peptides in Hydrated Media. VIII. Amino Acids with Aromatic Side Chains: L-phenylalanine, L-tyrosine, and L-tryptophan. *The Journal of Physical Chemistry B* **2010,** *114* (46), 15319-15330.
28. Nucci, N. V.; Scott, J. N.; Vanderkooi, J. M. Coupling of Complex Aromatic Ring Vibrations to Solvent through Hydrogen Bonds: Effect of Varied on-ring and off-ring Hydrogen-Bonding Substitutions. *The Journal of Physical Chemistry B* **2008,** *112* (13), 4022-4035.
29. Petoral Jr, R. M.; Uvdal, K. Arg–Cys and Arg–cysteamine Adsorbed on Gold and the G-protein–adsorbate Interaction. *Colloids and Surfaces B: Biointerfaces* **2002,** *25* (4), 335-346.
30. Uvdal, K.; Vikinge, T. Chemisorption of the Dipeptide Arg-Cys on a Gold Surface and the Selectivity of G-protein Adsorption. *Langmuir* **2001,** *17* (6), 2008-2012.